

Dielectric Relaxation and Charge Trapping Characteristics Study in Germanium Based MOS Devices With $\text{HfO}_2/\text{Dy}_2\text{O}_3$ Gate Stacks

Md. Shahinur Rahman, *Member, IEEE*, and Evangelos K. Evangelou, *Member, IEEE*

Abstract—In this paper, we investigate the dielectric relaxation effects and charge-trapping characteristics of $\text{HfO}_2/\text{Dy}_2\text{O}_3$ gate stacks grown on Ge substrates. The metal-oxide-semiconductor devices have been subjected to constant voltage stress (CVS) conditions at accumulation and show relaxation effects in the whole range of applied stress voltages. Applied voltage polarities, as well as thickness dependence of the relaxation effects, have been investigated. Charge trapping is negligible at low stress fields, whereas, at higher fields (> 4 MV/cm), it becomes significant. In addition, we give experimental evidence that, in tandem with the dielectric relaxation effect, another mechanism—the so-called Maxwell-Wagner instability—is present and affects the transient current during the application of a CVS pulse. This instability is also found to be field dependent, thus resulting in a trapped charge that is negative at low stress fields but changes to positive at higher fields.

Index Terms—Charge trapping, current decay, dielectric relaxation, Dy_2O_3 , gate stacks, germanium (Ge), HfO_2 , high- κ dielectrics, Maxwell-Wagner instability (M-W).

I. INTRODUCTION

AS GERMANIUM (Ge) offers higher mobility for electrons and holes when compared to silicon (Si), it draws extra attention in the semiconductor industry. In order to keep up with the scaling requirements set by the International Technology Roadmap for Semiconductors, gate dielectrics with higher permittivity ($\kappa \sim 25$), such as HfO_2 , is used as a replacement of SiO_2 [1]. Germanium is highly reactive with HfO_2 , which may lead to Ge diffusion into the HfO_2 dielectric [1]. One possible solution is the use of rare earth oxide dielectrics as interfacial buffer layers, which are “friendly” and can be directly deposited on Ge demonstrating better passivating and electrical properties [2]. Dy_2O_3 can efficiently eliminate Ge diffusion originating from either the substrate or

the interfacial layer, and also reduces charge-trapping effects while improving the equivalent oxide thickness (EOT) [3].

Another serious problem that arises when gate stacks of high- κ dielectrics are used in MOS devices is that they all produce electrical instabilities in the corresponding devices. As a result, anomalous threshold voltage (V_{TH}) shifts [4] are observed. It also raises reliability concerns as it affects drive currents with the time of operation. The position and spatial distribution of these traps are also very important. Most of them lie in the bulk of the oxides and show dramatic transient effects in the drain current of MOS field-effect transistor devices [5] or the leakage current of simple MOS capacitors [6]. In addition, when these traps lie close to the semiconductor–insulator interface, they may respond to the applied ac signals, thus leading to the concept of “border traps,” as introduced by Chen *et al.* [3], [7]. Moreover, all thin-film dielectrics are definitely far from being considered good insulators. While the use of relatively thicker high- κ dielectrics, instead of thin SiO_2 , is a considerable improvement, these films still conduct dc current, following one of the well-known current conduction mechanisms [8]. Therefore, when a dc voltage is applied on the gate electrode of a MOS capacitor, one of the following is likely to happen to gate current J_g .

- 1) Leakage current J_g increases, showing a charging capacitor behavior until—in a steady-state condition—no more defects are available to trap carriers.
- 2) Leakage current J_g increases (stress-induced leakage current, SILC), under bias condition [at high constant voltage stress (CVS)], due to the creation of new neutral defects in the bulk of the oxides.
- 3) When the defects lie close to the semiconductor or the metal gate electrode and/or their density and the capture cross section is high, the fast initial charging leads to significant reduction in the field across the dielectric, which is experimentally observed as a decay of J_g with time.

High- κ dielectrics are “trap-rich” materials [9]–[11], and charge trapping precludes accurate extraction of mobility of the devices [11], [12]. The crucial concern is to understand why charge trapping takes place in gate-stack dielectrics. It has been widely accepted that the trapped charge resides in localized electronic states associated with structural defects [11], [13]–[18], preexisting bulk defects [11], [19], dangling bonds at Ge-semiconductor/dielectric interface [20], oxygen vacancy, and deviancies [21]. No matter what the origin is or whether

Manuscript received May 13, 2011; revised July 4, 2011; accepted July 7, 2011. Date of publication August 18, 2011; date of current version September 21, 2011. The work of M. S. Rahman was supported in part by a Greek State Scholarship (IKY) and the MC-PAD postdoctoral fellowship. The review of this paper was arranged by Editor J. S. Suehle.

M. S. Rahman is with GSI-Helmholtz Zentrum für Schwerionenforschung, 64291 Darmstadt, Germany, and also with the OncoRay-Medical Faculty, University of Technology-Dresden, 01307 Dresden, Germany (e-mail: M.S.Rahman@gsi.de; Shahinur.Rahman@OncoRay.de).

E. K. Evangelou is with the Department of Physics, University of Ioannina, 45110 Ioannina, Greece (e-mail: eevagel@uoi.gr).

Color versions of one or more of the figures in this paper are available online at <http://ieeexplore.ieee.org>.

Digital Object Identifier 10.1109/TED.2011.2162095

they are bulk or interfacial defects, they all give rise to transient gate currents with considerably high time constants.

Apart from these effects, which are commonly encountered in MOS devices with high- κ oxide dielectrics; two more effects are likely to provide evidence of another source of unwanted transient currents. Relaxation effects and M-W instability are both related to the multilayer structure of some gate dielectrics, as will be explained in the succeeding paragraphs.

In its simple form, a MOS capacitor with a bilayer gate stack is usually studied with a thin (medium- κ) insulating layer in direct contact with the semiconductor surface and a thicker high- κ oxide on top. The main reason for this structure is the experimentally proven and theoretically predicted fact that the most interesting high- κ oxides (e.g., HfO_2 or ZrO_2) for potential MOS devices produce very poor interfaces with a high density of electrically active defects. Thus, a medium- κ buffer layer is utilized to suppress these interfacial defects. However, the existence of a high- κ material introduces another undesirable effect: a relaxation current, which follows the direction of the applied external voltage gradient dV_g/dt [22]–[24]. In general, relaxation in a solid involves the recovery of strain when the stress conditions change [24]. When an external field is applied across a film, it separates the bound charges, thus resulting in polarization and a compensating internal field [25]. The physical nature of dielectric relaxation can be explained with a potential well model in terms of dipole orientation [26]. Dipoles, which are homogeneously distributed inside a material, are formed by localized defects and disorder due to a lack of crystallinity.

Recently, Jameson *et al.* [27] showed that the presence of a gate stack is itself one cause of charge trapping in the bulk of the dielectrics and/or at the interfaces between the two dielectrics and substrate-buffer layer. The problem has been recognized and was solved analytically many years ago [28]. It is due to the different insulating properties of the high- κ layers in the gate stack, which results in different conductivities of each layer. Therefore, when a gate bias is applied to the stack, charge drifts easily through the poorer insulating layer and accumulates at the interface of the two dielectrics. As a consequence, the field across each insulator changes, so that, after sufficient time has passed, the same current density flows through both layers. The effect, which was described initially by Maxwell [29] himself and later on by Wagner [30], is the so-called “Maxwell-Wagner polarization” and causes current instabilities in voltage-stressed dielectric stacks. This is due to charge accumulation at the interface of the two layers, which stimulates dielectric relaxation effects in each high- κ layer. As dielectric relaxation is a continual buildup of polarization, following the application of an electrical bias, it results in a transient displacement current through the dielectric. Therefore, this current instability due to “Maxwell-Wagner polarization” is also termed as “Maxwell-Wagner instability (M-W).”

The aforementioned effects are already known to produce current instabilities in MOS devices containing various gate dielectrics. They both give a $J_g \sim t^{-n}$ behavior, which is strongly voltage dependent [5], [22], [27]. Moreover, they are usually both present at the same time, making the corresponding analysis a very complex task. The main subject of this paper is related

TABLE I
SUMMARY OF GATE STACK DIELECTRICS DEPOSITED AT DIFFERENT NOMINAL THICKNESS AND TYPES OF Ge SUBSTRATES

Samples reference	Structures (compositions)
N1	Pt/HfO ₂ (10nm)/Dy ₂ O ₃ (1nm)/ <i>n</i> -Ge
P1	Pt/Dy ₂ O ₃ (10nm)/ <i>p</i> -Ge
P2	Pt/HfO ₂ (5nm)/Dy ₂ O ₃ (2nm)/ <i>p</i> -Ge
P3	Pt/HfO ₂ (8nm)/Dy ₂ O ₃ (2nm)/ <i>p</i> -Ge
P4	Pt/HfO ₂ (5nm)/Dy ₂ O ₃ (5nm)/ <i>p</i> -Ge

analysis of the reliability issues of MOS devices comprising a dielectric gate stack. The studied devices grown on both *p*- and *n*-Ge substrates have been subjected to CVS conditions at accumulation. The aim of this paper is to identify M-W and relaxation effects, as well as charge trapping at preexisting bulk oxide defects, and to discuss potential reliability problems in future MOS devices.

II. EXPERIMENTAL

Dy₂O₃/HfO₂ oxide stacks were prepared by atomic oxygen beam deposition on both *p*- and *n*-type Ge (100) substrates. Native oxide was desorbed *in situ* under ultra high vacuum (UHV) conditions by heating the substrate to 360 °C for 15 min until a (2 × 1) reconstruction appears in the (RHEED) pattern, indicating a clean (100) surface. Subsequently, the substrate was cooled down to 225 °C, where the oxide stacks were deposited. The surface was exposed to atomic O beams generated by a radio-frequency plasma source with simultaneous e-beam evaporation of Dy/Hf at a rate of about ~0.15 Å/s. The same gate stacks (HfO₂/Dy₂O₃) of different compositions (nominal thicknesses), as well as single-layer Dy₂O₃, were prepared on both *n*- and *p*-type Ge substrates for this paper, as shown in Table I. More details on the preparation and structural analysis of the devices can be found elsewhere [31]. Metal–insulator–semiconductor capacitors were prepared by shadow mask and e-beam evaporation of 30-nm-thick Pt electrodes to define circular dots that are 200 μm in diameter. The back ohmic contact was made using a eutectic InGa alloy.

The devices were subjected to electrical stress under CVS conditions at accumulation [10]. Successive stress cycles of different time intervals and at different gate voltages were applied by means of a Keithley 617 source/meter, which was also measuring the corresponding current versus time ($J_g - t$) curves. After each stress cycle, the gate bias was stopped in order to measure either the current–voltage ($J_g - V_g$) curves or the high-frequency ($f = 100$ kHz) capacitance–voltage ($C - V_g$) curve. This determined the flat-band voltage shift (ΔV_{FB}). The latter measurement was obtained by means of an Agilent 4284A LCR meter. For the $J - t$ characteristics measurements, the capacitors were always biased at accumulation, and the absolute values of the current density and bias voltage were used in this study to avoid complexity. Fresh devices were used for each stress measurement with an area of 3.14×10^{-4} cm².

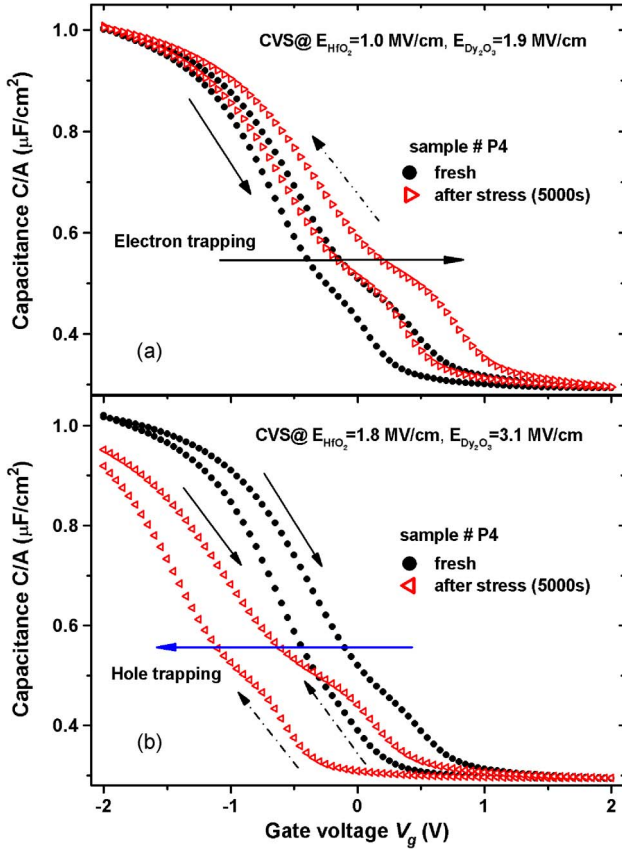


Fig. 1. (a) and (b) High-frequency $C-V_g$ ($f = 100$ kHz) curves on fresh and stressed devices of sample P4. Only the curve after the application of ten consecutive CVS cycles (500 s each) is plotted for clarity. Stress voltage is low in (a) and moderate in (b). Positive V_{FB} shifts in (a) indicate trapping of electron in the bulk of the oxides, whereas negative V_{FB} shifts in (b) indicate the creation of positively charged defects.

All the measurements were done in a dark box and at room temperature. The maximum change in temperature during the experiment was maintained within ± 0.2 °C.

III. RESULTS AND DISCUSSION

A. Capacitance–Voltage ($C-V$) Characteristics Under CVS

Typical $C-V_g$ curves of the MOS capacitors with gate stack dielectrics at low and moderate bias are illustrated in Fig. 1(a) and (b), respectively. In order to measure the trapped oxide charges immediately after stopping the stress pulse, the curves were obtained from accumulation to inversion and backward at a gate voltage sweep rate of $100 \text{ mV} \cdot \text{s}^{-1}$. This corresponded to switching times of ~ 40 s over the portion of the curve showing hysteresis. Ten successive CVS cycles of 500 s each were applied, and for the sake of clarity, the curves of the fresh device and after the tenth stress are shown in the figures. Nevertheless, the important electrical properties of the capacitors (e.g., the EOT or the density of interface states) do not show substantial differences from the $C-V_g$ acquired in the opposite way, which is typically used (i.e., from inversion to accumulation and backward). The hysteresis of the $C-V_g$ curves was rather large (about 400 mV at midgap), and a large density of slow interface traps is evident even at ac signal frequencies of as high as

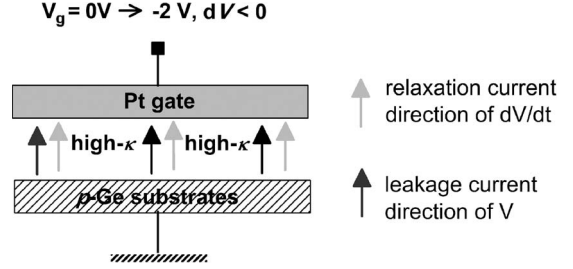


Fig. 2. Schematic diagram of the leakage and relaxation currents of an MOS device biased at accumulation.

100 kHz. The corresponding current–voltage (J_g-V_g) curves show very small leakage currents (about $15 \text{ nA/cm}^2 @ \pm 1 \text{ V} - V_{FB}$) [31].

The interesting result from the analysis of the high-frequency $C-V_g$ curves of sample P4 [Fig. 1(a) and (b)] is that, when the applied stress voltage is rather low, i.e., $V_g = -2 \text{ V}$ ($E_{HfO_2} = 1.0 \text{ MV/cm}$, $E_{Dy_2O_3} = 1.9 \text{ MV/cm}$), the trapped charge in the oxide is negative (i.e., ΔV_{FB} shift is positive). However, at moderate stress voltages, i.e., $V_g = -3 \text{ V}$ ($E_{HfO_2} = 1.8 \text{ MV/cm}$, $E_{Dy_2O_3} = 3.1 \text{ MV/cm}$), the observed negative shift of the $C-V_g$ curves indicates positive charge trapping. Similar results have been observed on all other gate stacks (see Table I), and there are two possible explanations for the observed phenomenon: First, as the gate voltage during the stress pulse is always negative, electrons are injected into the dielectrics from the metal. At low voltages, these electrons are trapped in preexisting defects, and the fields across each dielectric are not high enough for these electrons to escape toward the $p\text{-Ge}$ substrate. At higher stress voltages, the situation is different as holes are injected from the $p\text{-Ge}$ substrate into the oxide, thus resulting in the positive charge trapping. In addition, at the same time, a significant amount of new positive defects are created in the bulk of the oxides.

A different approach is to take into consideration the fact that, because the conductivities of HfO_2 and Dy_2O_3 thin films depend differently on the applied field, either layer can have the higher conductivity, depending on the choice of gate voltage. Frohman-Bentchkowsky and Lenzlinger [28] caused the sign of the trapped charge to switch by varying the gate voltage of similar (gate stack) structures. This effect was predicted from the independent measurements of the conductivities of the two layers [27], [28]. Similar changes of sign might have already been observed in HfO_2/SiO_2 gate stacks [28]. Furthermore, in previous work [10], we observed and reported the same effect on MOS devices with CeO_2 as the gate dielectric.

In order to check which of the aforementioned mechanisms is responsible for the observed V_{FB} shifts, the transient currents that are present during the application of a CVS pulse were measured. The corresponding analysis is presented in the succeeding paragraphs.

B. Voltage Dependence of Dielectric Relaxation

1) *Substrate Dependence of $J_g - t$ Curves:* As the direction of the leakage and relaxation currents depend on the polarities

TABLE II
CALCULATION OF THE APPLIED GATE VOLTAGES AND THE CORRESPONDING ELECTRIC FIELDS
ACCORDING TO (2) AND (3) FOR SAMPLES (a) P2 AND (b) N1 AT TIME $t = 0$ s

Fig. 3(a) sample #P2			Fig. 3(b) sample #N1		
Gate voltage (V)	Corresponding fields across gate stacks (MV/cm)		Gate voltage (V)	Corresponding fields across gate stacks (MV/cm)	
$-V_g$	E_{HfO_2}	$E_{\text{Dy}_2\text{O}_3}$	V_g	E_{HfO_2}	$E_{\text{Dy}_2\text{O}_3}$
0.7	0.6	1.1	1.7	1.4	2.5
1.4	1.4	2.6	2.2	1.9	3.3
2.1	2.3	4.0	2.8	2.3	4.2
2.8	3.1	5.8	3.3	2.8	5.0
3.5	3.9	6.9	3.9	3.3	5.8
4.1	4.5	8.1	4.4	3.7	6.7
4.2	4.7	8.4	4.8	4.1	7.3
			5.3	4.5	8.0

of V and dV , respectively, their magnitude can be either additive or subtractive. The directions of these two currents through the high- κ gate stack of a p -Ge-based device are illustrated in Fig. 2. When a negative gate voltage pulse is applied, the device is driven in accumulation, and the relevant leakage current is negative. At the same time, as $dV < 0$, the magnitude of the relaxation current is also negative.

In order to study the current transient characteristics of both n - and p -Ge-based MOS devices, we applied different CVS bias (from $|1|$ to $|5|$ V) on samples P2 and N1, and the corresponding fields are given in Table II. The corresponding current densities as a function of stress time ($J_g - t$) curves are shown in Fig. 3(a) and (b). Interestingly, on p -Ge-based devices and low-CVS conditions, a decaying current, which follows a power law (t^{-n}), is observed [see Fig. 3(a)]. For the gate stacks grown on n -type substrates, this current decay is never traceable, even at very low CVS conditions [see Fig. 3(b)]. On the contrary, at higher stress voltages and on both types of substrates, we do not notice dielectric relaxation because of the dominating charge-trapping mechanism, which will be discussed in a later section. Soft breakdown (SBD) and hard breakdown (HBD) events have also been detected at higher fields and/or prolonged time stress [Fig. 3(a)].

In order to better understand which mechanism is responsible for the change in direction of the ΔV_{FB} shift with the applied gate voltage, the transient response of the current during the application of the stress pulse was monitored in more detail [see Fig. 1(a) and (b)]. Fig. 4 illustrates the current density J_g versus stress time t curves after the application of relatively moderate stress voltages on p -Ge-based devices (in the form of train pulses). During the CVS measurement, we recorded the $J_g - t$ curves after the application of ten consecutive stress pulses, each one having a duration of 500 s while the gate voltage was kept constant [10]. Between the voltage pulses, $J_g - V_g$ curves at accumulation were also acquired. In Fig. 4, only the first and last curves are plotted for the sake of clarity. The decay of J_g follows a t^{-n} law, with n values varying smoothly from 0.73 to a value of $n = 0.91$ after ten successive stress cycles. The fact that the initial n value is far from unity indicates that a M-W instability (following the terminology used in [27]) is likely to be present, together with the usual dielectric relaxation of the high- κ dielectrics. In the latter case, the relaxation current decays with

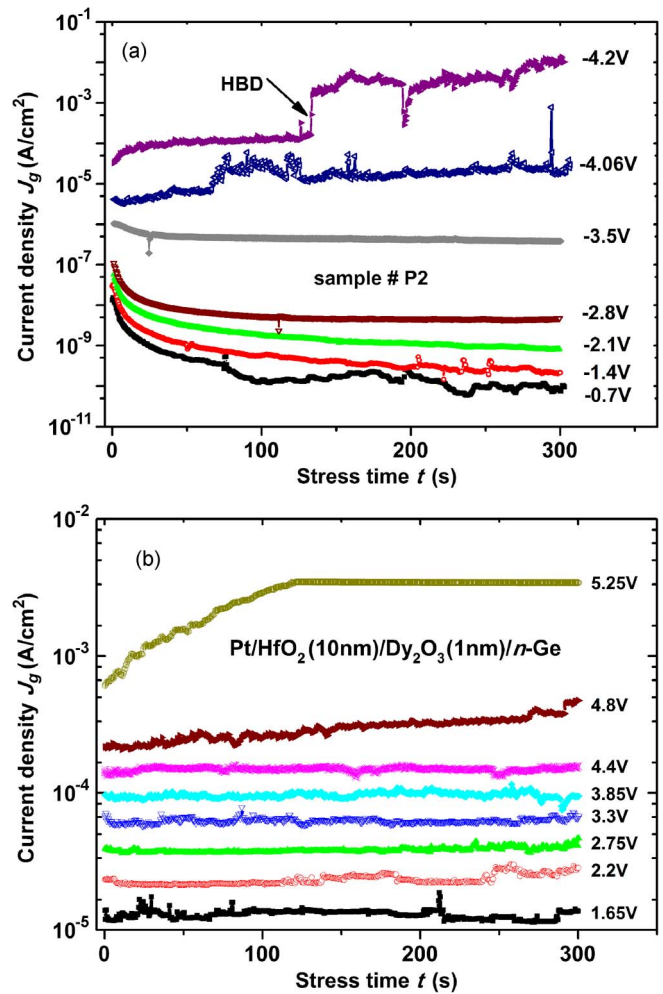


Fig. 3. (a) and (b) Current density as a function of stress time curves ($J_g - t$) at different CVS conditions of a gate stack grown on (a) p - and (b) n -type Germanium substrates (samples P2 and N1, respectively). The corresponding fields across each dielectric are given in Table II.

time, following the Curie-von Schweidler (C-S) relaxation law [24], i.e.,

$$J_e = C \cdot t^{-n} \quad (1)$$

where J_e is the relaxation current density (in amperes per square centimeter). $C = P \cdot \alpha$, where P is the total polarization

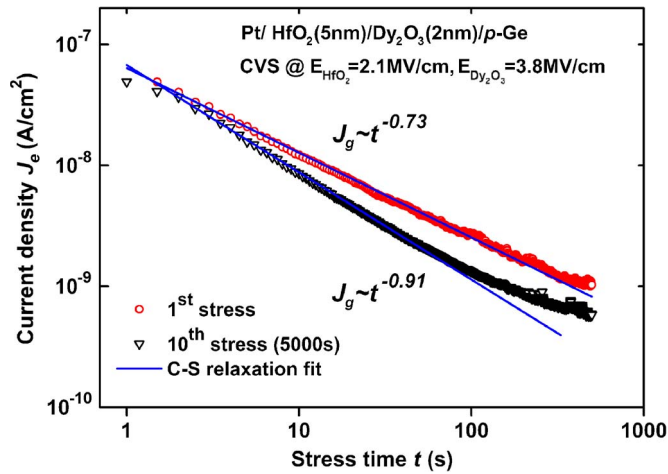


Fig. 4. Absolute values of current density (J_g) as a function of stress time t . The transient current behavior during the application of the first and tenth stress pulses is shown for clarity. The change in slope is rather smooth for the corresponding curves obtained during the application of intermediate CVS pulses (i.e., second to ninth). The applied stress field is low for this gate stack configuration (sample P2). Solid lines represent the C-S relaxation t^{-n} fit to the experimental data.

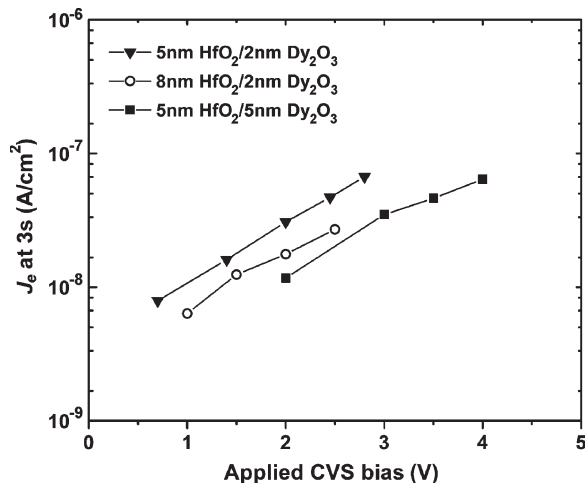


Fig. 5. Gate relaxation current measured 3 s after setting the stress pulse for three different gate stacks (HfO₂/Dy₂O₃/p-Ge), as a function of applied CVS bias voltage. The gate stacks were grown on p -type Ge substrates, and the applied CVS bias was negative, i.e., at accumulation. The relaxation current changes linearly with V_g and is thickness dependent.

or surface charge density (in volt-nanofarad per square centimeter), α is a constant in seconds, and n is a real number close to unity. The gradual increase in n could be attributed to the fact that the M-W becomes less important after each stress cycle. The relevant J_e values decrease, so that, after ten consecutive cycles, the dielectric relaxation current dominates. One possible explanation for this effect is the gradual change in the conductivities of the two dielectric layers, due to charge trapping on preexisting bulk oxide defects.

2) *Thickness Dependence of Dielectric Relaxation:* Fig. 5 shows that the relaxation current increases linearly with increasing gate bias for three different gate stack configurations (samples P2, P3, and P4). The current measured at $t = 3$ s ($J_{g=3s}$), after setting the stress pulse, is used as a measure of the amplitude of the relaxation current. From (1), the magnitude

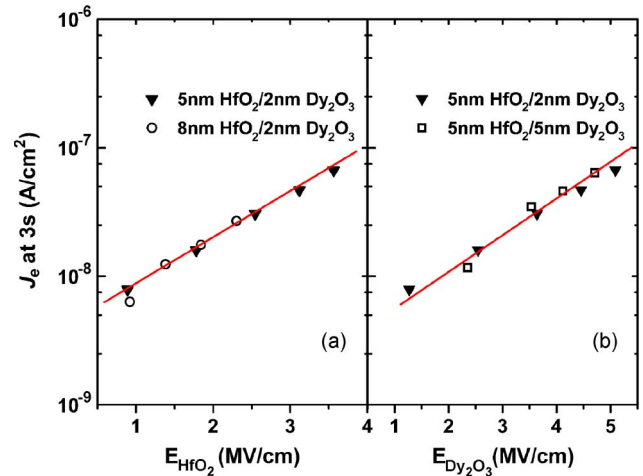


Fig. 6. (a) and (b) Gate relaxation current measured at 3 s as a function of (a) HfO₂ high- κ and (b) Dy₂O₃ interfacial layer electric fields in p -substrate MOS capacitors. Relaxation current is thickness independent on HfO₂ or Dy₂O₃ electric fields that anticipates the polarization model and is incompatible to the charge-trapping/detrapping model. The solid lines are simply a guide to the eye.

of the relaxation current is directly proportional to the applied voltage across the dielectric. Therefore, a linear J_g - V_g plot indicates the presence of relaxation currents rather than any other transient mechanisms. It should be noted here that, due to rise time limitations of the measuring instrument, the J_g data acquired for $t < 1$ s are not taken into account. Jameson *et al.* [27], Reisinger *et al.* [32], and Luo *et al.* [22] observed similar current decays on Si-based devices, which were attributed to the relaxation of the dielectric material, whereas Xu *et al.* [33], and Bachhofer *et al.* [34] explained these effects by charge trapping-detrapping within the gate dielectrics.

In order to explain which of the preceding models apply to our results, relaxation current densities (J_e) at 3 s as a function of the electric field across (a) HfO₂ and (b) Dy₂O₃ are plotted in Fig. 6(a) and (b). From the figures, there is a clear indication of the thickness independence of the relaxation current. This is expected as the amplitude of polarization is controlled by the electric field across the dielectric materials. As a result, the corresponding current should be identical when induced by the same electric field and independent of the film thickness variation [24]. Similar results have been reported by Reisinger *et al.* in BSTO [32] films. This thickness independence is consistent with the normal dielectric material polarization model [24], [35] and cannot be explained by charge trapping and detrapping mechanisms [33]. As V_g is negative, the electrons are injected from the gate electrode. This means that the calculations of the initial electric fields across the HfO₂ and Dy₂O₃ films are very important factors. The field across each of the layers of the gate stack can be calculated as [36]

$$E_{\text{HfO}_2} = \frac{V}{(\kappa_1/\kappa_2)d_2 + d_1} \quad (2)$$

$$E_{\text{Dy}_2\text{O}_3} = \frac{V}{(\kappa_2/\kappa_1)d_1 + d_2} \quad (3)$$

where $V = V_g - V_{\text{FB}} - \Psi_s$ is the voltage applied to the gate dielectric stack, V_{FB} is the flat-band voltage, and Ψ_s is the

initial surface potential of Ge. $d_{1,2}$ is the thickness of the high- κ (HfO₂) or the interfacial (Dy₂O₃) layer, respectively, with κ_1 and κ_2 being their dielectric constants, respectively. All field values in this paper were calculated using (2) and (3). It should be pointed out that the calculation of the initial electric field in the high- κ film, i.e., HfO₂ (2), as well as the initial field across Dy₂O₃ (3), is only an estimation of the magnitudes and will be discussed in the next section.

C. Correlation of Dielectric Relaxation and M-W

As has been discussed earlier, because of the bilayer structure, some charge is accumulated at the interface between the two dielectrics due to the M-W instability [27]. In addition, if one tries to fit the experimental $J_g - t$ data by means of the C-S law alone, the calculated values of n are less than unity ($n \sim 0.73$). However, after successive CVS cycles (i.e., continuous charge injection), this value of n tends to unity ($n = 0.91$), which could be explained if one assumes that the relaxation effects and the “M-W” act simultaneously. According to the potential well model [26], the current due to relaxation from a single dielectric layer is

$$J_g = 2\sigma_0 \frac{V}{d} \left(3 + \ln \frac{t}{t_{0,1}} \right) \frac{t_{0,1}}{t} t > t_{0,1} \quad (4a)$$

where V is the applied external bias, d is the thickness of the dielectric, whereas t_o and σ_0 are material constants. In general, t_o is expected to be on the order of picoseconds, whereas σ_0 is not related to the dc conductivity of the insulating oxide layer. In the case of a gate stack configuration, where the two dielectrics are perfect insulators, the field across each dielectric will be different than the simple V/d factor of (4a).

However, the first dielectric (k_1 in Fig. 2), which is deposited on top of the semiconductor surface, is usually very thin and mainly amorphous. It is then reasonable to assume that it does not contribute to the relaxation current. However, it does modify the field across the top dielectric, and an M-W factor is introduced. Therefore, the relaxation current due to these combined effects can be expressed as [27]

$$J_g = 2E_{\text{HfO}_2} \sigma_{0,1} \left(3 + \ln \frac{t}{t_{0,1}} \right) \frac{t_{0,1}}{t}, t > t_{0,1} \quad (4b)$$

where

$$E_{\text{HfO}_2} = \frac{V\kappa_2}{d_1\kappa_2 + d_2\kappa_1}$$

is the field across the high- k material (HfO₂ in this case); $\sigma_{0,1}$ and $t_{0,1}$ are the material constants that set the scale of current and time, respectively, and all other terms have been mentioned before in (2) and (3).

At this point, it is interesting to notice that (4b) could only be utilized for the present gate stacks under the following assumptions:

- 1) The REO buffer layer is thin and amorphous, so that the corresponding relaxation effects are suppressed. Otherwise, a second term (which accounts for the relaxation in the buffer layer) must be added in (4b).

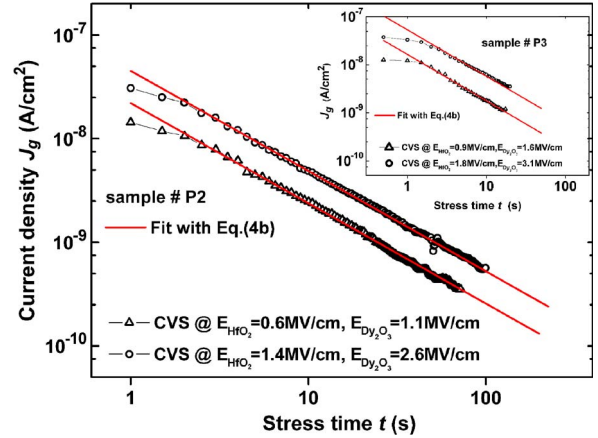


Fig. 7. Gate current as a function of stress time of two different thicknesses gate stacks (P2 and P3). Solid lines are best fit to (4b) and indicate that the combined effect of relaxation and M-W better describes the observed current decay.

- 2) Equation (4b) could only fit the experimental $J - t$ data for a short time interval (usually < 100 s) as it does not take into account leakage current effects.
- 3) The field E_{HfO_2} across HfO₂ may differ from $V\kappa_2/(d_1\kappa_2 + d_2\kappa_1)$ by an amount depending on the magnitude of the interfacial charge σ , as explained in detail in [26]. One way to obtain accurate interfacial charge (σ) values is the use of correct conductivities $J_1(E_1)$ and $J_2(E_2)$. Without knowledge of the conductivity of each dielectric layer, $V\kappa_2/(d_1\kappa_2 + d_2\kappa_1)$ is only an approximation, which is based on the fact that the relevant change in the field across each dielectric is small. The conductivity could be approximated by a linear (i.e., ohmic) behavior.

The aforementioned prerequisites could not be met in all samples and stress voltages used in this study. Thus, the model was only used to explain the deviation from the Curie von Schweidler ($J \sim t^{-1}$) law.

Fig. 7 shows the current density as a function of stress time at different low gate voltages. It should be mentioned here that the use of the gate voltage V_g as the changing parameter was chosen in many plots in this paper. This was done as the use of the corresponding fields [by means of (2) and (3)] turns out to be very complicated. We fit the experimental data for two different thicknesses of HfO₂/Dy₂O₃ gate stacks and two different V_g values using (4b). The thickness of each layer is obtained from independent measurements, whereas V , J , and t are derived from experimental data. Therefore, in order to find the values of the free running parameters $\sigma_{0,1}$, $t_{0,1}$, and $\kappa_{1,2}$, two different sets of experimental $J - t$ data were acquired after application of different V_g voltages on the same sample. Fitting (4b) to the experimental data, the relevant parameters have been calculated as $\kappa_1 = 20$, $\kappa_2 = 13$, $\sigma_{0,1} = 2 \sim 3 \times 10^{-5}$ A/cm², and $t_{0,1} = 2.1 \times 10^{-11}$ s, respectively. It should be noted here that an accurate solution of the four unknown parameters of (4) needs a set of four $J = f(V_g, t)$ equations. However, the separation of parameters in (4) and the initial guess values for $\sigma_{0,1}$ and $t_{0,1}$ obtained from similar analyses in [27] was proven to be good enough for the excellent fit shown in Fig. 7(a) and (b). The

TABLE III
DIELECTRIC CONSTANT (κ VALUES) AND EOT VALUES OF HfO_2 , Dy_2O_3 , AND $\text{HfO}_2/\text{Dy}_2\text{O}_3$ GATE STACKS, FROM A FIT OF (4b) TO THE EXPERIMENTAL DATA AND AFTER A RECENT STUDY [31] OF HIGH-FREQUENCY C - V CURVES

$\text{HfO}_2/\text{Dy}_2\text{O}_3$ gate stacks					experimental results for single HfO_2 or Dy_2O_3 layers	EOT				
present study		C - V measurement (ref.31)				$\text{HfO}_2/\text{Dy}_2\text{O}_3$ gate stacks (ref.31)				
K_{HfO_2}	$K_{\text{Dy}_2\text{O}_3}$	K_{HfO_2}	$K_{\text{Dy}_2\text{O}_3}$	Effective K (gate stacks)	K_{HfO_2} (ref.37)	$K_{\text{Dy}_2\text{O}_3}$ (ref.38)	P1	P2	P3	P4
20	13	23~25	13~14	16~18	20~25	12~14	2.68	1.93	2.29	2.77

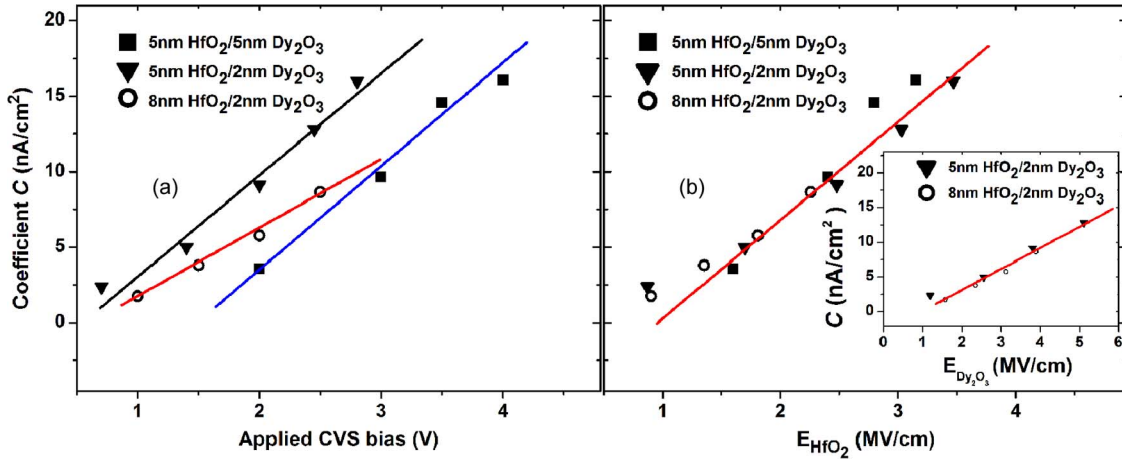


Fig. 8. (a) and (b) Experimental results of the dielectric relaxation current in high- k $\text{Pt}/\text{HfO}_2/\text{Dy}_2\text{O}_3/\text{p-Ge}$ gate stacks. (a) Coefficient C in fits of C/t^n to the dielectric relaxation current of gate stack capacitors biased into accumulation (V_g negative). (b) Same data as in (a) but with the horizontal axis scaled in $E_{\text{HfO}_2} = V\kappa_2/d_1\kappa_2 + d_2\kappa_1$ according to (4), making the data collapse onto a single line. C versus $E_{\text{Dy}_2\text{O}_3}$ data are shown as an inset in Fig. 8(b). The solid lines are simply a guide to the eye.

addition of two more $J = f(V_g, t)$ experimental curves does not alter the obtained values significantly.

Comparable κ values of HfO_2 [37] and Dy_2O_3 [38] have been confirmed by means of high-frequency C - V measurements [31] on similar samples (see Table III). Therefore, it should be emphasized here that the κ values obtained after fitting (4b) to the experimental data is another measure of the validity of the model described by (4b) under the relevant assumptions. Furthermore, in an attempt to fit a simple relaxation power law ($J_e \sim t^{-n}$) to the experimental data of moderate to high applied V_g values [see Fig. 4], the obtained exponent value deviated considerably from unity. In addition, the exponent n was never the same during the first stress cycle when slightly different stress voltages were applied to the same sample. It was then reasonable to assume that the current decay was not due to relaxation effects alone. On the contrary, when the applied CVS values were lower than 1.5 V, the relaxation effects dominate, and the use of (4b) explains the deviation of the exponent n from unity.

In order to show the validity of (4b), for the case of a gate stack configuration, one can check it against a set of various thicknesses of the two oxides. After fitting the experimental data using (1) (when bias is applied to the MOS capacitors) corresponding preexponential factor C as a function of gate bias is illustrated in Fig. 8(a). The variation of thickness for both the high- κ and interfacial layers results in notably different C lines, as shown in Fig. 8(a). However, when the time-independent

coefficients of (1) and (4b) are considered, coefficient C is equal to $C = 2E_{\text{HfO}_2}\sigma_{0,1}$, whereas the time-dependent terms of both equations are practically indistinguishable. Coefficient C versus the field across the high- κ dielectric (E_{HfO_2}) is plotted in Fig. 8(b). Experimental data in this case lie one on top of another. This figure illustrates that this scaling holds true, meaning that the thickness dependence of (4b) is correct for the case where the thickness of the interfacial layer varies (2–5 nm), whereas that of the high- κ layer is held fixed. Moreover, the thickness dependence of (4b) is also correct when the thickness of the interfacial layer is held fixed, whereas that of HfO_2 varies (5–8 nm) [see Fig. 8(b) “insert”]. Jameson *et al.* [27] reported similar results for $\text{HfO}_2/\text{SiO}_2$ -based devices on p -Si substrates.

D. Dielectric Relaxation and Charge-Trapping Characteristics at Higher Stress Voltages

The application of higher stress voltages on the same MOS devices results in quite different transient characteristics of the corresponding $J_g - t$ curves. As illustrated in Fig. 9(a), upon application of moderate to high stress voltages, i.e., $V_g = -4.8$ V ($E_{\text{Dy}_2\text{O}_3} = 4.8$ MV/cm) on the single- Dy_2O_3 devices, the relaxation effects disappear. The transient current behavior is now governed by charge trapping at preexisting bulk oxide defects. In contrast, application of moderate stress voltages, i.e., $V_g = -3.0$ V ($E_{\text{HfO}_2} = 3.3$ MV/cm, $E_{\text{Dy}_2\text{O}_3} = 5.9$ MV/cm) on capacitors with the $\text{HfO}_2/\text{Dy}_2\text{O}_3$ stack (Fig. 9(b), sample

P2), shows the coexistence of two different mechanisms separated only by the different time scales of each one. Therefore, during the first 32 s after the application of the pulse, the current density J_g decreases with time due to the relaxation mechanisms. This follows a t^{-n} law with n values of as low as 0.6. At the same time, the magnitude of the leakage current that flows through the dielectrics is two to three orders of magnitude higher than in the case of low stress voltages [see, e.g., Figs. 4 and 7(a)]. Therefore, the charge-trapping effects become more significant, and the J_e values start to increase, following a model originally proposed by Nigam *et al.* [39] to explain charge trapping in MOS devices with thin gate stack dielectrics [40]:

$$J_g - J_o = N^+(V_g) \cdot \left[1 - e^{-\frac{t}{\tau}} \right] + \alpha \cdot t^\nu \quad (5)$$

with $N^+(V_g)$ being the saturation value of positive charge trapping, τ being the trapping time constant, and α and ν being the SILC-related parameters, and J_o being the first value of current density. The first term in (5) represents an exponentially saturating charge buildup on preexisting oxide defects, whereas the second term represents the increase due to SILC generation.

According to (5), the transient behavior of J_g with time [for sample P1, see Fig. 9(a)] could be explained by taking into consideration both trapping on preexisting bulk oxide defects (with a characteristic time constant $\tau \sim 32$ s) and creation of new defects due to electrical stressing [which follow a power law $J_g \sim t^\nu$, as in (5)]. However, for sample P2, only charge trapping was considered for best fitting of the experimental data [see Fig. 9(b)]. In addition, time constant τ is one order of magnitude greater ($\tau \sim 260$ s) for that device than for the structure containing only Dy_2O_3 . This is an interesting result as it shows that there are different types of defects in the two oxides. Furthermore, the overall better insulating properties of HfO_2 are confirmed. Sample P2, although stressed at slightly higher electric fields, shows negligible rate of creation of new defects. Similar effects have been observed for the other devices with bilayer dielectrics studied in this paper, as illustrated in Fig. 9(c). In this figure, the existence of both SBD and HBD effects is clearly demonstrated for moderate- to high-CVS conditions.

IV. CONCLUSION

The charge-trapping and relaxation characteristics of $\text{Pt}/\text{HfO}_2/\text{Dy}_2\text{O}_3/\text{Ge}$ gate stacks have been studied by means of CVS measurements. At low applied stress voltages, two independent electrical instabilities have been observed, i.e., the M-W and dielectric relaxation. While both effects were present simultaneously, the increase in the applied voltage and/or the repetition of the stress cycles led to a change in the relative magnitude of each one separately. Another aspect of the studied structures worth noting is that, because of the different effects dominating at low to medium or high applied fields, the sign of the trapped charge switched from positive to negative, which is an effect that has been rarely reported for high- κ gate stacks. Finally, at moderate- to high-stress fields, the dominant process is charge trapping and creation of new defects (SILC). The

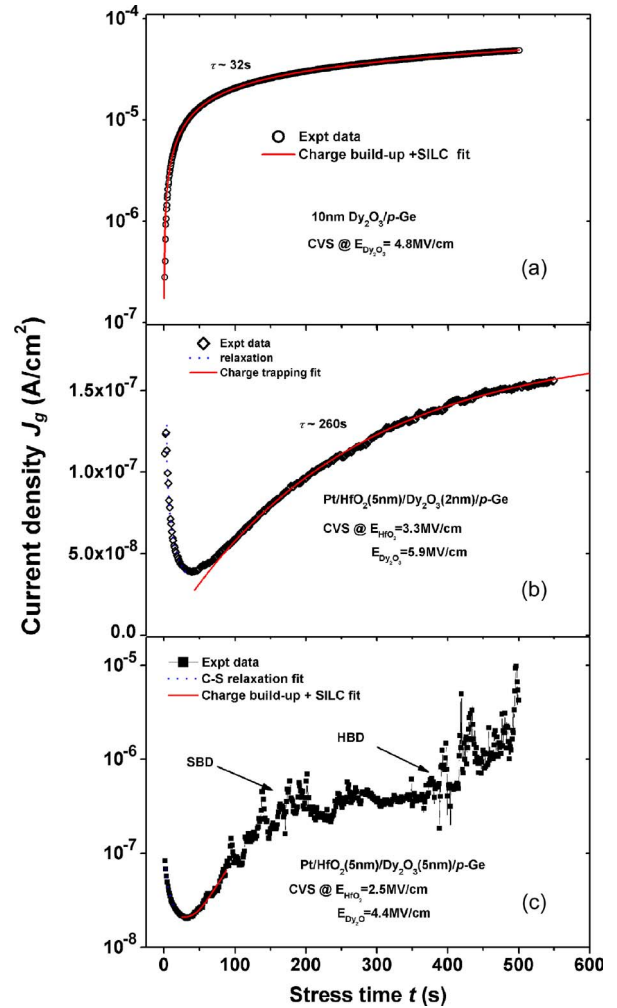


Fig. 9. (a)–(c) $|J_g|$ versus t curves are shown, when the applied gate voltages are rather high, so that the corresponding fields are moderate for all samples P1, P2, and P4 [(a)–(c) respectively]. The solid lines are best fit to the experimental data according to (5).

analysis of the transient behavior of the current density in this case revealed the existence of two different trapping centers in the two dielectrics at least in terms of the relevant capture cross sections.

ACKNOWLEDGMENT

The authors would like to thank Dr. R. Perrin for reading the whole manuscript and for the valuable suggestions and corrections, and Dr. A. Dimoulas for providing the samples.

REFERENCES

- [1] C. O. Chui, S. Ramanathan, B. B. Triplett, P. C. McIntyre, and K. C. Saraswat, "Germanium MOS capacitors incorporating ultrathin high- κ gate dielectric," *IEEE Electron Device Lett.*, vol. 23, no. 8, pp. 473–475, Aug. 2002.
- [2] A. Dimoulas, "Electrically active interface and bulk Semiconductor defects in high- k /germanium structures," in *Defects in High- k Gate Dielectric Stacks*, vol. 220. New York: Springer-Verlag, 2006, pp. 237–248.
- [3] D. K. Chen, R. D. Schrimpf, D. M. Fleetwood, K. F. Galloway, S. T. Pantelides, A. Dimoulas, G. Mavrou, A. Sotiropoulos, and Y. Panayiotatos, "Total dose response of Ge MOS capacitors with $\text{HfO}_2/\text{Dy}_2\text{O}_3$ gate stacks," *IEEE Trans. Nucl. Sci.*, vol. 54, no. 4, pp. 971–974, Aug. 2007.

- [4] A. Toriumi and T. Nabatame, "Anomalous V_{FB} shifts in high- k gate stacks—Is its origin at the top or bottom interface?" *ECS Trans.*, vol. 25, no. 6, pp. 3–16, 2009.
- [5] A. Kerber, E. Cartier, L. Pantisano, R. Degraeve, T. Kauerauf, Y. Kim, A. Hou, G. Groeseneken, H. E. Maes, and U. Schwalke, "Origin of the threshold voltage instability in $\text{SiO}_2/\text{HfO}_2$ dual layer gate dielectrics," *IEEE Electron Device Lett.*, vol. 24, no. 2, pp. 87–89, Feb. 2003.
- [6] S. Hall, O. Bui, and Y. Lu, "Direct observation of anomalous positive charge and electron-trapping dynamics in high- k films using pulsed-MOS-capacitor measurements," *IEEE Trans. Electron Devices*, vol. 54, no. 2, pp. 272–278, Feb. 2007.
- [7] D. M. Fleetwood, "'Border traps' in MOS devices," *IEEE Trans. Nucl. Sci.*, vol. 39, no. 2, pp. 269–271, Apr. 1992.
- [8] D. Schroder, *Semiconductor Material and Device Characterization*, 2nd ed. New York: Wiley, 1998.
- [9] M. Houssa, A. Stesmans, M. Naili, and M. M. Heyns, "Charge trapping in very thin high-permittivity gate dielectric layers," *Appl. Phys. Lett.*, vol. 77, no. 8, pp. 1381–1383, Aug. 2000.
- [10] M. S. Rahman, E. K. Evangelou, A. Dimoulas, G. Mavrou, and S. Galata, "Anomalous charge trapping dynamics in cerium oxide grown on germanium substrate," *J. Appl. Phys.*, vol. 103, no. 6, p. 064 514, Mar. 2008.
- [11] S. Zafar, A. Callegari, E. P. Gusev, and M. V. Fischetti, "Charge trapping related threshold voltage instabilities in high permittivity gate dielectric stacks," *J. Appl. Phys.*, vol. 93, no. 11, pp. 9298–9303, Jun. 2003.
- [12] E. P. Gusev, C. D'Emic, S. Zafar, and A. Kumar, "Charge trapping and detrapping in HfO_2 high- κ gate stacks," *Microelectron. Eng.*, vol. 72, no. 1–4, pp. 273–277, Apr. 2004.
- [13] L. Pantisano, E. Cartier, A. Kerber, R. Degraeve, M. Lorenzini, M. Rosmeulen, G. Groeseneken, and H. E. Maes, "Dynamics of threshold voltage instability in stacked high- κ dielectrics: Role of the interfacial oxide," in *VLSI Symp. Tech. Dig.*, 2003, pp. 159–160.
- [14] S. Zafar, A. Callegari, E. Gusev, and M. V. Fischetti, "Charge trapping in high- κ gate dielectric stacks," in *IEDM Tech. Dig.*, 2002, pp. 517–520.
- [15] R. Degraeve, T. Kauerauf, A. Kerber, E. Cartier, B. Govoreanu, P. Roussel, L. Pantisano, P. Blomme, B. Kaczer, and G. Groeseneken, "Stress polarity dependence of degradation and breakdown of $\text{SiO}_2/\text{high-}\kappa$ stacks," in *Proc. 41st Int. Reliab. Phys. Symp.*, 2003, pp. 23–28.
- [16] J. C. Wang, S. H. Chiao, C. L. Lee, T. F. Lei, Y. M. Lin, M. F. Wang, S. C. Chen, C. H. Yu, and M. S. Liang, "A physical model for the hysteresis phenomenon of the ultrathin ZrO_2 film," *J. Appl. Phys.*, vol. 92, no. 7, pp. 3936–3940, Oct. 2002.
- [17] E. P. Gusev, D. A. Buchanan, E. Cartier, A. Kumar, D. DiMaria, S. Guha, A. Callegari, S. Zafar, P. C. Jamison, D. A. Neumayer, M. Copel, M. A. Gribelyuk, H. Okorn-Schmidt, C. D'Emic, P. Kozlowski, K. Chan, N. Bojarczuk, L.-A. Ragnarsson, P. Ronsheim, K. Rim, R. J. Fleming, A. Mocuta, and A. Ajmera, "Ultrathin high- κ gate stacks for advanced CMOS devices," in *IEDM Tech. Dig.*, 2001, pp. 451–454.
- [18] A. Cester, A. Paccagnella, and G. Ghidini, "Time decay of stress-induced leakage current in the thin gate oxides by low-field electron injection," *Solid State Electron.*, vol. 45, no. 8, pp. 1345–1353, Aug. 2001.
- [19] N. A. Chowdhury, G. Bersuker, C. Young, R. Choi, S. Krishnan, and D. Misra, "Breakdown characteristics of nFETs in inversion with metal/ HfO_2 gate stacks," *Microelectron. Eng.*, vol. 85, no. 1, pp. 27–35, Jan. 2008.
- [20] M. Houssa, G. Pourtois, M. Caymax, M. Meuris, M. M. Heyns, V. V. Afanas'ev, and A. Stesmans, "Ge dangling bonds at the (100) Ge/GeO_2 interface and the viscoelastic properties of GeO_2 ," *Appl. Phys. Lett.*, vol. 93, no. 16, p. 161 909, Oct. 2008.
- [21] K. Tse, D. Liu, K. Xiong, and J. Robertson, "Oxygen vacancies in high- κ oxides," *Microelectron. Eng.*, vol. 84, no. 9/10, pp. 2028–2031, Sep./Oct. 2007.
- [22] W. Luo, Y. Kuo, and W. Kuo, "Dielectric relaxation and breakdown detection of doped tantalum oxide high- κ thin films," *IEEE Trans. Device Mater. Rel.*, vol. 4, no. 3, pp. 488–494, Sep. 2004.
- [23] G. G. Raju, *Dielectrics in Electric Fields*. New York: Marcel Dekker, 2003.
- [24] A. K. Jonscher, "Dielectric relaxation in solids," *J. Phys. D, Appl. Phys.*, vol. 32, no. 14, pp. R57–R70, 1999.
- [25] M. Schumacher and R. Waser, "Curie-von Schweidler behavior observed in ferroelectric thin films and comparison to superparaelectric thin film materials," *Integr. Ferroelectr.*, vol. 22, pp. 109–121, 1998.
- [26] J. R. Jameson, W. Harrison, P. B. Griffin, and J. D. Plummer, "Double-well model of dielectric relaxation current," *Appl. Phys. Lett.*, vol. 84, no. 18, pp. 3489–3491, May 2004.
- [27] J. R. Jameson, P. B. Griffin, J. D. Plummer, and Y. Nishi, "Charge trapping in high- κ gate stacks due to the bilayer structure itself," *IEEE Trans. Electron Devices*, vol. 53, no. 8, pp. 1858–1867, Aug. 2006.
- [28] D. Frohman-Bentchkowsky and M. Lenzlinger, "Charge transport and storage in Metal-Nitride-Oxide-Silicon (MOS) structures," *J. Appl. Phys.*, vol. 40, no. 8, pp. 3307–3319, Jul. 1969.
- [29] J. C. Maxwell, *Electricity and Magnetism*, vol. 1. Oxford, U.K.: Clarendon, 1892.
- [30] K. W. Wagner, *Die Isolierstoffe der Elektrotechnik*, H. Schering, Ed. Berlin, Germany: Springer-Verlag, 1924.
- [31] E. K. Evangelou, M. S. Rahman, I. I. Androulidakis, A. Dimoulas, G. Mavrou, K. P. Giannakopoulos, D. F. Anagnostopoulos, R. Valicu, and G. L. Borchert, "Structural and electrical properties of $\text{HfO}_2/\text{Dy}_2\text{O}_3$ gate stacks on Ge substrates," *Thin Solid Films*, vol. 518, no. 14, pp. 3964–3971, May 2010.
- [32] H. Reisinger, G. Steinlesberger, S. Jakschik, M. Gutsche, T. Hecht, M. Leonhard, U. Schroder, H. Seidl, and D. Schumann, "A comparative study of dielectric relaxation losses in alternative dielectrics," in *IEDM Tech. Dig.*, 2001, pp. 12.2.1–12.2.4.
- [33] Z. Xu, L. Pantisano, A. Kerber, R. Degraeve, E. Cartier, S. De Gendt, M. Heyns, and G. Groeseneken, "A study of relaxation current in high- κ dielectric stacks," *IEEE Trans. Electron Devices*, vol. 51, no. 3, pp. 402–408, Mar. 2004.
- [34] H. Bachhofer, H. Reisinger, E. Bertagnolli, and H. von Philipsborn, "Transient conduction in multielectric silicon-oxide-nitride-oxide semiconductor structures," *J. Appl. Phys.*, vol. 89, no. 5, pp. 2791–2800, Mar. 2001.
- [35] H. Frohlich, *Theory of Dielectrics*. London, U.K.: Oxford Univ. Press, 1958.
- [36] M. S. Rahman, E. K. Evangelou, I. I. Androulidakis, and A. Dimoulas, "Current transport mechanism in high- κ cerium oxide gate dielectrics grown on Germanium (Ge)," *Electrochem. Solid-State Lett.*, vol. 12, no. 5, pp. H165–H168, Feb. 2009.
- [37] A. Dimoulas, G. Mavrou, G. Vellianitis, E. K. Evangelou, N. Boukos, M. Houssa, and M. Caymax, " HfO_2 high- κ gate dielectrics on Ge (100) by atomic oxygen beam deposition," *Appl. Phys. Lett.*, vol. 86, no. 3, p. 032 908, Jan. 2005.
- [38] T. Lee, S. J. Rhee, C. Y. Kang, F. Zhu, H.-S. Kim, C. Choi, I. Ok, M. Zhang, S. Krishnan, G. Thareja, and J. C. Lee, "Structural advantage for the EOT scaling and improved electron channel mobility by incorporating dysprosium oxide (Dy_2O_3) into HfO_2 n -MOSFETs," *IEEE Electron Device Lett.*, vol. 27, no. 8, pp. 640–643, Aug. 2006.
- [39] T. Nigam, R. Degraeve, G. Groeseneken, M. M. Heyns, and H. Maes, "A fast and simple methodology for lifetime prediction of ultra-thin oxides," in *Proc. 37th Int. Reliab. Phys. Symp.*, 1999, pp. 381–388.
- [40] E. K. Evangelou, M. S. Rahman, and A. Dimoulas, "Correlation of charge buildup and stress-induced leakage current in cerium oxide films grown on Ge (100) substrates," *IEEE Trans. Electron Devices*, vol. 56, no. 3, pp. 309–407, Mar. 2009.



Md. Shahinur Rahman (S'06–M'09) was born in Narail, Bangladesh. He received the B.Sc. (honors) and M.Sc. degrees in physics from the University of Dhaka, Dhaka, Bangladesh, in 2000 and 2002, respectively, and the Ph.D. degree from the University of Ioannina, Ioannina, Greece, in 2009. His thesis was focused on the electrical characteristics and reliability issues of high- κ rare earth oxide gate dielectrics on germanium MOS devices.

He has been continuing his research, after his doctoral study, under a Marie Curie Fellowship, i.e.,

MCPAD (Postdoctoral research) of CERN, and has been with the Detector Laboratory, GSI-Helmholtzzentrum für Schwerionenforschung, Darmstadt, Germany, working on chemical-vapor-deposition diamond detectors. Recently, he has also been a Semiconductor Radiation Detectors Expert with the OncoRay-Medical Faculty, University of Technology-Dresden, Dresden, Germany, in collaboration with the Department of Radiation Physics, Helmholtzzentrum Dresden Rossendorf (HZDR). His current research interests include compound semiconductor detectors, Compton cameras, cancer therapy with radiation ion beams, radiation damage/defects in materials, detector physics and particle detectors (e.g., diamond detectors), dielectric/oxide defects and electrical characterization, reliability issues of CMOS devices, Ge-based MOS devices with high- κ dielectrics, and rare earth oxides as high- κ gate dielectrics.

Dr. Rahman was awarded the Greek-state Ph.D. fellowship (IKY), a postgraduate scholarship from the University of Dhaka, and the Bangladesh Sena-Kallan scholarship (undergraduate and postgraduate). He was the recipient of the "IEEE RS Scholarship 2009" from the IEEE Reliability Society.



Evangelos K. Evangelou (M'01) received the B.A. and Ph.D. degrees in physics, for his research on defects in III-V-based semiconductor devices, from the University of Ioannina, Ioannina, Greece, in 1985 and 1994, respectively.

He spent a year as a Research Fellow with the Opto-electronic Devices Group, Department of Electrical and Electronic Engineering, The Nottingham Trent University, Nottingham, U.K., where he worked on the electrical characterization of ACTFEL devices. In 1996, he joined the Department of Physics, University of Ioannina, where he is currently an Assistant Professor. Since 2000, he has participated in several research projects with different industrial partners (ST Microelectronics and IMEC) and research centers (NCSR "Demokritos," MDM-INFM), aiming to study novel high- k materials for potential use in future MOS devices. His current research interests include the electronic properties of Ge-based MOS devices, as well as the reliability issues of novel MOS devices with high- k dielectrics.